Ideal ballooning modes in the ASDEX-Upgrade, JET and TCV pedestals

M. G. Dunne[1], L. Frassinetti[2], B. Lomanowski[3], U. Sheikh[4], N. Vianello[5], E. Wolfrum[1], L. Radovanovic[6], I. S. Carvalho[7], D. Frigione[8], L. Garzotti[9], B. Labit[4], M. Maslov[9], F. G. Rimini[9], G. Sergienko[10], P. A. Schneider[1], D. van Eester[11], The ASDEX Upgrade Team*, The EUROfusion MST1 Team†, JET contributors††, the TCV Team‡

[1]*Max Planck Institute for Plasma Physics, Boltzmannstr. 2, 85748 Garching, Germany,* [2]*Division of Fusion Plasma Physics, KTH Royal Institute of Technology, Stockholm SE,* [3]*Oak Ridge National Laboratory, Oak Ridge, TN 37831, USA* [4]*Ecole Polytechnique Fédérale de Lausanne (EPFL), Swiss Plasma Center (SPC), Lausanne, Switzerland,* [5]*Consorzio RFX, Padova, Italy* [6]*Institute of Applied Physics, TU Wien, Fusion@ÖAW, 1040 Vienna, Austria,* [7]*Instituto de Plasmas e Fusão Nuclear, Instituto Superior Técnico, Universidade de Lisboa, 1049-001 Lisboa, Portugal,* [8]*Università di Roma Tor Vergata, Via del Politecnico 1, Roma, Italy,* [9]*United Kingdom Atomic Energy Authority, Culham Science Centre, Abingdon, Oxon, OX14 3DB, UK,* [10]*Forschungszentrum Jülich GmbH, Institut für Energie- und Klimaforschung, Plasmaphysik, 52425 Jülich, Germany,* [11]*Laboratory for Plasma Physics LPP-ERM/KMS, B-1000 Brussels, Belgium,* **See author list of H. Meyer et al. 2019 Nucl. Fusion 59 112014,* †*See author list of B. Labit et al. 2019 Nucl. Fusion 59 086020,* ††*See the author list of 'Overview of JET results for optimising ITER operation' by J. Mailloux et al. to be published in Nuclear Fusion Special issue: Overview and Summary Papers from the 28th Fusion Energy Conference (Nice, France, 10-15 May 2021),* ‡*See author list of S. Coda et al. 2019 Nucl.Fusion 59 112023*

A complete understanding of pedestal structure and limits remains an open question in fusion research. Research in this direction generally makes use of some generalised version of the EPED model[1]; transport mechanisms (which can have different drives for the particles and heat, and for ions and electrons) determine, in combination with the heat and particle sources, the profile gradients. In the "standard" case, the profiles continue to extend radially further inwards away from the separatrix until there is enough free energy in the pressure gradient (and associated driven edge current density) that a large magnetohydrodynamic (MHD) instability occurs, the so-called edge localised modes (ELMs). The onset of the ELM then determines the steepest and widest pedestal pressure profile.

The onset of the ELM is often rather sudden, which has inspired the use of ideal MHD to describe the critical pre-ELM profiles. Many publications have shown good agreement between the peeling-ballooning (PB) model (coupled modes driven by the current density and pressure gradient) and experimental observations. More recent work on ASDEX Upgrade (AUG), JET-ILW, and TCV have shown the importance of the location of the pressure gradient profile relative to the separatrix; experiments shifting the density profile peak radially outwards show

significantly reduced performance, which is reproduced by the models).

Despite the general success of the PB model, there are some notable exceptions. Many, though by no means all, cases in JET with the ITER-like wall (Be main chamber and W divertor) do not agree with the predictions of PB, indicating that some physics must be missing[2]. In addition, recent work investigating the parameter space of no/small-ELM regimes[3] proposes a transport-limited pedestal, where a radially small mode close to the separatrix creates enough transport to hold the pedestal short of the PB limit. With these exceptions in mind, the aim of this work is to examine pedestal transport in combination with PB stability for the three devices, AUG, JET, and TCV.

While the determination of the active transport mechanism in the pedestal via gyrokinetic simulations remains open, there are two main hypotheses for modes which are expected in the pedestal: the kinetic ballooning mode (KBM), as proposed in the EPED model and; the electron temperature gradient (ETG) mode. Evidence for the latter was presented by Schneider et al.[4]; a constant average gradient length in the pedestal in three devices of ca. 2 cm.

The methodology followed here starts with fetching the pedestal profiles from each of the machines. Due to different data gathering, storage, and fitting methods at each machine, this is handled on a case-by-case basis. Once this is done, ”a self-consistent path” is created, following the strategy described in[5]. A single equilibrium representative of the time window in which the profiles are fitted is loaded (an exact equilibrium is not necessary at this point, as only the plasma boundary, an approximate q-profile, and the total stored energy are required). Using these experimental data as a base, the pedestal Te and Ti profiles are scaled up and down (assuming a constant density profile and fixed temperature pedestal width) to create a range of pedestal pressures.

For TCV and JET, the core profiles are scaled to match the experimental beta, for AUG the fast-ion content is calculated using the RABBIT code and added to the thermal profiles (which are well known for both ions and electrons across the full radius). Next, the edge current density is calculated self-consistently using the Redl model[6] and a parabolic core current is created to match the experimental plasma current. Finally, the range of pressure and current density profiles are used along with the plasma boundary as input to the HELENA equilibrium code (which also calculates the n=∞ stability profile) and finally to the MISHKA

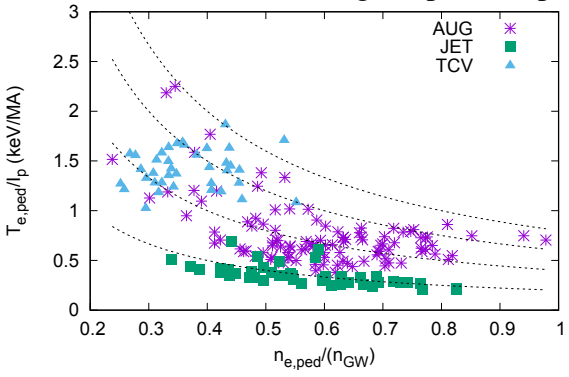

Figure 1: Normalised temperature vs normalised density for the three devices; AUG (purple), JET-ILW (green), and TCV (blue). The dashed lines depict lines of constant β_θ

ideal-MHD stability code for global pedestal stability.

To give an impression of the data set used for this study, a plot showing the pedestal top temperature normalised to the plasma current as a function of the pedestal top density normalised to the Greenwald density is shown in figure 1. This normalisation has the benefit of allowing lines of constant $\beta_{\theta,ped}$ to be over-plotted, demonstrating that the normalised pedestal height from the three machines overlaps reasonably well (though the JET-ILW data in this data set tend towards lower values than AUG or TCV; future extensions will attempt to remedy this).

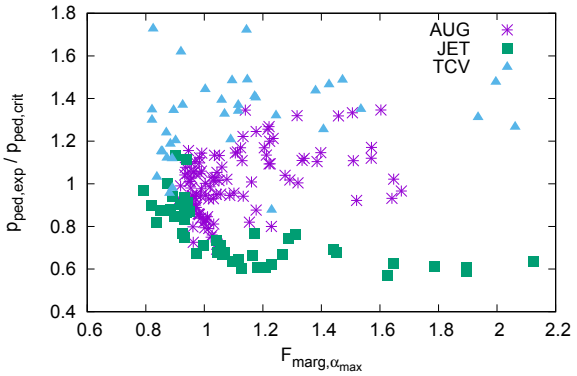

Figure 2: $p_{ped,exp}/p_{ped,crit,PB}$ vs $F_{marg,\alpha_{max}}$ for AUG, JET-ILW, and TCV. A clear trends of higher F_{marg} and increasing gap to the PB stability boundary can be seen for JET-ILW.

A starting hypothesis of this work centered around the idea that second stability access was necessary for good confinement; an example of this has already been presented for JET-ILW plasmas[7], showing that only plasmas with second stability access reached the PB boundary. We examined this here by comparing the peak value of F_{marg} (the ratio of the n=∞ critical α to the experimental one) to the distance to the PB boundary for all three devices. The result of this is shown in figure 2.

While the AUG and TCV data sets lie withing a reasonable distance to the PB boundary, it has already been seen that the JET-ILW data are relatively far away. One can also see that the JET-ILW plasmas have high values of F_{marg}, and the higher the value of F_{marg}, the further away these plasmas are from the PB boundary. A value of F_{marg} close to one (or second stability access) appears to be a necessary criterion for PB instability (one sees at high values of p_{exp}/p_{crit} an increase of F_{marg} again; this is due to local second stability access in the middle of the pedestal). This implies that if the pedestal transport is not governed by MHD-like mechanisms that it will not reach the PB boundary. This result may not be surprising, but the analysis here highlights the differences between JET-ILW and AUG/TCV for both PB stability **and** potential transport mechanisms.

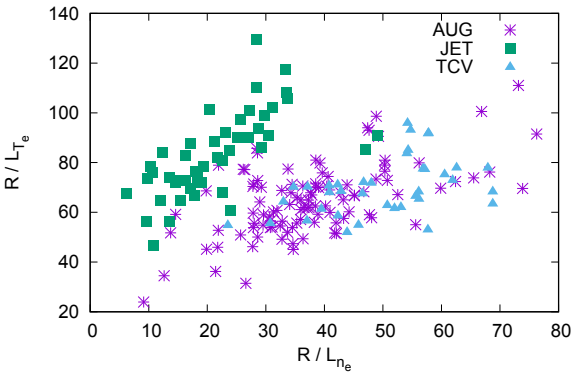

Figure 3: R/L_{T_e} vs R/L_{n_e} for AUG, JET-ILW, and TCV. While AUG and TCV overlap, JET-ILW pedestals exist at higher values of R/L_{T_e}.

Given the lack of PB instabilities or KBM/ideal-ballooning transport in the analysed JET-ILW plasmas, it is interesting to investigate other transport mechanisms, as already suggested in [2]. To this end, the gradient lengths of electron temperature and density averaged over the

pedestal width are shown for the three devices in figure 3. The gradients for this plot are taken as a function of $r_{minor,OMP}$; the general relations shown here do not change when taking the gradients against Ψ_N or any other normalised radius. While the AUG and TCV data lie on top of one another in this space, the JET data are notably shifted to higher R/L_{T_e}, implying higher transport (particularly for a given value of L_{n_e}). It should be noted in addition that although a high separatrix density (or high L_{n_e}, see figure 4, which is strongly correlated) is observed in each device to degrade confinement, it does not necessarily provide a correlation to the departure from the PB boundary.

In conclusion, the implemented workflow allows a comparison of pedestal stability across multiple devices. The study has highlighted key areas in which the AUG and JET-ILW data sets presented here could be easily extended to improve overlap (notably towards higher $n_{e,sep}/n_{e,ped}$ in AUG and lower $n_{e,sep}/n_{e,ped}$ in JET-ILW); the present data sets were chosen simply for practical reasons of an established data set in AUG and divertor diagnostic coverage in JET-ILW. These data exist on both devices, but have not yet been included in the analysis.

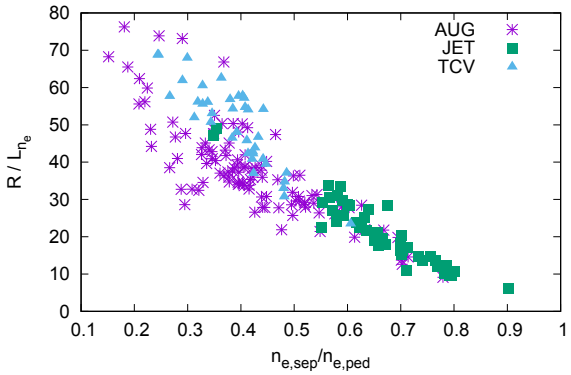

Figure 4: $n_{e,sep}/n_{e,ped}$ vs R/L_{n_e} for AUG, JET-ILW, and TCV.

The comparison of distance to the PB boundary with the local ballooning stability margin highlights the importance of understanding the transport in the pedestal not only for predictive purposes, but also for maximising performance. The JET-ILW data set, which exhibits higher transport when compared to AUG and TCV, exists at lower $\beta_{\theta,ped}$ and further away from the stability boundary. Given the strong link between divertor conditions and the $n_{e,sep}/n_{e,ped}$ ratio (or, alternatively, and perhaps more importantly, the density gradient length) known from all three devices, this indicates that the density pedestal is key to understanding the overall pedestal structure and stability.

References

[1] P. B. Snyder, et al. *Physics of Plasmas*, 16(5), 2009.

[2] L. Frassinetti. *IAEA FEC*, 2021.

[3] G F Harrer, et al. *Nuclear Fusion*, 58(11), 2018.

[4] P.A. Schneider, et al. *Plasma Physics and Controlled Fusion*, 56(2), 2014.

[5] S. Saarelma, et al. *Physics of Plasmas*, 22(5), 2015.

[6] A. Redl, et al. *Physics of Plasmas*, 28(2), 2021.

[7] C. Bowman, et al. *Nuclear Fusion*, 58(1), 2018.

This work has been carried out within the framework of the EUROfusion Consortium and has received funding from the Euratom research and training programme 2014-2018 and 2019-2020 under grant agreement No 633053. The views and opinions expressed herein do not necessarily reflect those of the European Commission. This work was supported in part by the Swiss National Science Foundation.